



## Oceanic loading monitored by ground-based tiltmeters at Cherbourg (France)

Nicolas Florsch, Muriel Llubes, Guy Wöppelmann, Laurent Longuevergne,  
Jean-Paul Boy

### ► To cite this version:

Nicolas Florsch, Muriel Llubes, Guy Wöppelmann, Laurent Longuevergne, Jean-Paul Boy. Oceanic loading monitored by ground-based tiltmeters at Cherbourg (France). Journal of Geodynamics, 2009, 48, pp.211-218. 10.1016/J.JOG.2009.09.017 . hal-00708017

HAL Id: hal-00708017

<https://hal.science/hal-00708017>

Submitted on 14 Jun 2012

**HAL** is a multi-disciplinary open access archive for the deposit and dissemination of scientific research documents, whether they are published or not. The documents may come from teaching and research institutions in France or abroad, or from public or private research centers.

L'archive ouverte pluridisciplinaire **HAL**, est destinée au dépôt et à la diffusion de documents scientifiques de niveau recherche, publiés ou non, émanant des établissements d'enseignement et de recherche français ou étrangers, des laboratoires publics ou privés.

1   **Oceanic loading monitored by ground-based tilt-meters**

2   **at Cherbourg (France)**

3

4   Nicolas Florsch<sup>(\*)</sup><sup>(1)</sup>, Muriel Llubes<sup>(2)</sup>, Guy Wöppelmann<sup>(3)</sup>, Laurent Longuevergne<sup>(4)</sup>, Jean-

5   Paul Boy<sup>(5)</sup>

6

7   (1) UMMISCO/IRD 32, avenue Henri Varagnat 93143 Bondy Cedex, France; UPMC,

8       Paris, France; Dept of Mathematics and Applied Mathematics, UCT, South Africa.

9   (2) Université de Toulouse, OMP 14 av. Edouard Belin, 31400 Toulouse, France

10   (3) LIENSs/ULR, 2 rue Olympe de Gouges, 17000 La Rochelle , France

11   (4) Bureau of Economic Geology, Jackson School of Geosciences, The University of

12       Texas at Austin, PO Box X, Austin, TX 78713, USA

13

14   (5) EOST/IPGS (UMR 7516 CNRS-ULP), 5 rue René Descartes, 67084 Strasbourg,

15       France, and NASA GSFC, Planetary Geodynamics Laboratory, Code 698,

16       Greenbelt, MD 20771, USA.

17

18

19    **Abstract**

20    We installed two orthogonal Blum-Esnoult silica tiltmeters in an underground military facility  
21    close to the shore in Cherbourg (France). They have recorded the ocean tide and the  
22    associated oceanic loading effects from March 2004 to July 2005. The signal to noise ratio is  
23    such that, within a period range from a few minutes to a few days, the main nonlinear oceanic  
24    tides up to the M10 group could be observed. The modelling of the tidal tilt deformation has  
25    been carried out using oceanic models of the FES2004 family, with a stepwise refinement of  
26    the grid size. The comparison with recorded tilt time series shows spectacular improvement  
27    when refining the grid and also provides an independent mean to validate the oceanic models  
28    and the modelling process. We show that tiltmeters open new opportunities to explore loading  
29    of non linear tides on a larger spectrum than gravimeters and GPS do.

30    **Keywords**

31    Inclinometry, tilt, oceanic loading, FES2004, nonlinear tides

32    **1. Introduction**

33    The oceanic loading phenomenon involves the attraction and deformation of the Earth that are  
34    due to the varying weight of moving water masses in the oceans and seas, mainly the oceanic  
35    tides. These effects may be measured on the ground by several geodetic observables:  
36    classically gravity, land level displacement, (Llubes, 2001, Vey, 2002, Llubes, 2008), but also  
37    strain and stress can be used.

38    This paper is focused on to the tilt effects generated by tidal oceanic loading on the French  
39    coast (Cherbourg, Cotentin region). The tidal amplitude may reach there up to several meters.

40 While considering gravity variations in the vicinity of a sea with large tides, the proper  
41 loading contribution can reach about the third of the elastic earth tide variation (Llubes et al.,  
42 2004). Tilts are much more sensitive to the coastal loading because they result mainly from  
43 the flexure of the crust, which involves a sensitivity to shorter spatial scales than gravimetry  
44 does. Actually the tilt loading itself reaches at Cherbourg about three times the solid tide tilt  
45 effect. Precisely, two factors converge to generate a large amplitude to the loading tilt *locally*:  
46 1) The decreasing rate of the tilt Green function as a function of the load distance is more  
47 rapid with respect to gravity: it behaves as  $1/r^2$  instead of  $1/r$ . This feature leads to a sort of  
48 homothetic invariance scale (Rerolle et al., 2006) when integrating over an area which also  
49 depends on  $r^2$ ; 2) Coastal areas are zones where the tidal amplitude is much greater than in the  
50 open ocean. Finally, these properties make the tiltmeters highly sensitive and suitable to  
51 study local loading phenomena.

52 Strictly speaking, tiltmeters record the variations of the gravity direction, more precisely the  
53 variations between the instantaneous geoid and the crust on which these instruments are  
54 settled. Both are affected by water loads. In practical terms, the only signal that can be  
55 reached is the difference between the geoid and the crust. It is not possible to refer tilts to a  
56 space or terrestrial reference frame because the accuracy that would be required to refer tilt  
57 data to this frame should be of the same order of magnitude than a tiltmeter resolution (at  
58 least), that is better than  $10^{-9}$  at short time scale (a few seconds). Of course, it is only a  
59 practical limitation. Actually, the zero instrumental reference is just its initial state when  
60 beginning the record.

61 The geometrical and dynamical effects induced by the oceanic loads can be easily computed  
62 using the Green formalism, which degenerates in a simple convolutive formalism as long as  
63 the Earth is considered as spherically symmetric. Green functions describe the linear elastic  
64 Earth response to a local load in terms of vertical and horizontal displacements, stress, strain,

65 gravity... Tilt Green functions can be found in Pagiatakis (1990). See also Boy et al. in this  
66 issue.

67 **2. Experiment description and site corrections**

68 **2.1. Tiltmeters records**

69 The tiltmeters used in this experiment are very compact instruments historically designed by  
70 Blum (1962) (see also Saleh, 1991) and nowadays built by Marie-France Esnoult at IPGP.  
71 These instruments are made with silica glass and is built according to Zöllner's pendulum  
72 concept. Tiltmeters require a two-step calibration: the first one is electronic (the sensitivity of  
73 the displacement probe) and the second one is purely mechanistic (the amplification of a  
74 pendulum is  $1/\sin(\alpha)$ ,  $\alpha$  being the angle between the rotation axe and the vertical line).

75 Scientific and historical background of this kind of probes may be found in Melchior (1983).  
76 Braitenberg et al. (1999) also provide a suitable summary of their functioning.

77

78 The tiltmeters used in this experiment can reach a resolution of about  $10^{-9}$  rad. Actually the  
79 gain accuracy (calibration constant) is expected to be better than 4 % (at  $1\sigma$ ). However,  
80 pendulums are affected by some "external" limitations. They are highly sensitive to very local  
81 environmental background variations: temperature, humidity of the supporting materials, and  
82 any kind of natural or induced deformation of the stand. For instance, assuming a 30 cm  
83 baseline tripod, a 1 micrometer stem vertical displacement would lead to a  $3.10^{-6}$  rad tilt  
84 effect. Generally speaking, a noticeable drift is observed on that kind of instruments, which is  
85 rarely understood in details. This drift could also involve the creeping of the tiltmeter  
86 components themselves: it is worth mentioning that  $10^{-9}$  rad variation over a 30 cm baseline is  
87 less than the elementary quartz crystal size. Hence, a suitable efficiency can only be reached

88 thanks to exceptional settling conditions. In our experiment, two orthogonal pendulums have  
89 been installed in an unused part of a military underground installation owned by the French  
90 Marine, the “Souterrain du Roule”, at Cherbourg (Figure 1). A drift does actually exist on  
91 both tiltmeters directions (EW and NS). However, it only causes interferences within the long  
92 period variations (saying, more than a week), which can be eliminated by standard filtering  
93 methods to focus on the diurnal tidal band and its harmonics without spectral windowing  
94 artefacts.

95 **2.2. Site effects**

96 Site effects include both topographic and cavity effects. Both deform the local stress field and  
97 so they modify (magnify or reduce) the targeted tilt signal. Harrison (1976) was the first to  
98 provide a useful approach to deal with such undesirable effects. He clearly showed the major  
99 influence of the topography: in the core of a hill, the tilt could be changed by a large factor  
100 (from 0.25 to 10 outdoor in a talweg). An essential characteristic of site effects is the relative  
101 phase shift with respect to its theoretical value, which can reach as much as 40° (Lecolazet  
102 and Wittlinger, 1974).

103 The paper by King *et al.* mentions two issues to correct the site effects: first the practical  
104 problem of constructing and checking large three-dimensional models, and second the  
105 difficulties of obtaining the correct input data for the models. Nowadays, Finite Element  
106 Method (FEM) could be applied (see for instance Kroner *et al.* 2005). However, in our case it  
107 will not be very useful. These authors also remind us Itsueli *et al.* work (1975) in which the  
108 problem of the existence of surrounding fracture - that are not well mapped introduces  
109 additional difficulties. They proposed a method for removing the site effects without recourse  
110 to modelling by using a response method actually based on the seismic response or Raleigh  
111 waves. Neither of these methods can be used here. As stated by King et al (1976) the first

112 method is valid only for sites distant from ocean loading and the second requires at least the  
113 vertical component which is not available in our case.

114 However two points must be emphasised to lower the site effects. Firstly, body forces are  
115 generally considered to study cavity effects, whereas the study of the crust flexure results  
116 from remote surface loads. Potential site effects are reduced to a shear effect alone. Here, the  
117 direct Newtonian attraction is lowered (water masses are more or less at the same altitude than  
118 the instrument) –however, the mass redistribution potential (and forces) cannot be neglected.  
119 Secondly, tiltmeters have been installed more or less in the middle of the tunnel (a symmetry  
120 axis), where the disturbing effect is supposed to vanish.

121 The solution we finally adopted consists in dropping potential site effect corrections,  
122 assuming it is less critical than in the frame of a body Earth Tide study. Finally, remembering  
123 that Lecolazet and Wittlinger (1974) associated a significant phase to cavity effect, we state  
124 that the undetectable phase difference between the observed and the modeled tidal tilt  
125 variations will be an a-posteriori justification of the reduced rule of site effect.

126 **2.3. Atmospheric contribution on tilt.**

127 The atmosphere contributes to the tilt as any other moving mass (Boy *et al*, this issue). Two  
128 deformation processes have to be modeled: direct attraction (modifying the equipotential),  
129 and the elastic deformation due to the additional pressure on the crust, which also implies  
130 mass redistribution and thus an effect on the geoid (Farrell, 1972). The formalism to compute  
131 the atmospheric contribution is similar to those used in the oceanic or continental  
132 (hydrological) loading problems, except that one should consider here that the station is inside  
133 the atmosphere shell. As in the hydrological case, tilts are only influenced by the spatial  
134 pressure gradient (Rerolle *et al.*, 2006). It implies that the classical admittance method cannot  
135 be used in our case. Two methods can be used to correct the atmospheric pressure

contribution. One would use a local barometer network, which would require a heavy installation structure because of the different spatial scales involved in the deformation. A test was carried out, but did not provide good results. Moreover, the pressure effect on that coastal border is complicated by the dynamic response of the ocean. The second method consists in using the atmospheric data as provided by meteorological models. Unfortunately, the sampling rate of these is too coarse, and does not allow to study phenomena below 12 hours. On a spectral point of view, pressure effects induce a rosy noise superimposed with periodic signals. If a good atmospheric pressure correction is expected to improve the S/N ratio, we suspect that it would be a real but light improvement in our spectral analysis. Finally, we dropped this correction since no data is available within the given frequency range.

Traditional Earth Tide (ET) studies have benefited from gravity observations, such as the GGP experiment (<http://www.eas.slu.edu/GGP/ggphome.html>). Most of the geodesists consider that the discrepancies between the observations and the models are very tiny. Actually, they are much smaller toward the inner continental stations where the influence of oceanic loadings is reduced. The agreement between the Love numbers used to compute Earth elastic tides and the GGP cryogenic gravimeter data is better than 1/100. This is indeed negligible when considering the factor calibration accuracy and one can assume that the modelled Earth tide elastic contribution is very accurate and can be subtracted from the raw data to leave only oceanic loading effects. However, the situation is not so simple if we remind the nature of the site effect. Here, an “exact tide” is subtracted from a signal where the tides could have been multiplicatively changed by the site magnification. Hence, the legitimacy to remove the elastic tide lies on the fact that i) it is smaller than the loading, ii) the site effect factor is not too far from 1 (due to the location of the probes near the center of the tunnels). The combination of these two “small” hypothesis let us hope that these approximations are not too dramatic, although it is not possible to estimate them with

161 accuracy. Finally, we consider that the error associated with site effects is reduced due to (1)  
162 the position of the tiltmeters in the center of the tunnel and (2) the reduced amplitude of the  
163 Earth Tide by a factor 5 with respect to loading.

164 **3. Signal processing and spectral analysis.**

165 **3.1 Basic spectral analysis**

166 Tilts were initially sampled at 30 sec intervals. We applied high-pass filtering (to remove the  
167 drift) and resampling (with low-pass filtering to avoid aliasing). This finally restricts the  
168 bandwidth to the useful periods between 10minutes and 72 hours. Raw and filtered signals are  
169 plotted on Figure 2. The amplitude spectra of the filtered signals are plotted on Figure 3. We  
170 chose a spectral normalization which preserves the amplitude of the periodic signal rather  
171 than the density power spectrum. Hence, the tidal wave amplitudes can be directly read in  
172 microradians.

173 The spectra show several harmonics of the diurnal tidal waves. They are directly linked to the  
174 non-linear hydrodynamical waves in the English Channel (and do not result from any kind of  
175 non-linearity of the Earth elastic response). The most further way to model the observed  
176 amplitude requires to compute these non linear waves by using the most complete oceanic  
177 charts (involving hydrodynamic modelling plus data assimilation) and to combine them with  
178 the rheological response of the Earth (convolutive or more sophisticated). However, the  
179 difficulties of getting upper order waves lies in the mesh definition and restitution as seen by  
180 altimetric satellites, more exactly it depends on the trade-off between time and space  
181 sampling, both limited in practice (Cartwright and Ray, 1990). This becomes more and fussier  
182 as the order increases, since the higher the order, the smaller the typical wavelength to be  
183 taken into account.

184 Several points should be highlighted here:

185 - the amplitude of even orders is greater than for other harmonics. This is expected  
186 since they are successive harmonics of the M2 dominant group.

187 - Tiltmeters are able to record nonlinear waves up to 8 cycle/day. Note that neither  
188 loading gravity studies (Boy *et al.*, 2004) nor any other integrative geodetic method  
189 have been able to “see” these higher harmonic signals (although they are clearly seen  
190 in tide gauge records, of course). Hence tiltmeters turns out to be very sensitive tools  
191 to observe the deformation induced by the oceanic tides at the regional scale.

192

### 193 **3.2. Tidal analysis**

194 Earth tide analysis softwares are designed to estimate the transfer response of the Earth with  
195 respect to the astronomical gravity potential, usually providing the delta and gamma factors  
196 (Melchior, 1983). To search for higher tidal harmonics in the tiltmeter records, we therefore  
197 looked for tidal analysis tools which actually are standard within the sea-level community.

198 We used the MAS software developed by Simon (2007) which implements a general method  
199 for analysing sea level heights. Povreau *et al.* (2006) compared MAS to the well-known and  
200 widely distributed T\_TIDE software (Pawlowicz *et al.* 2002), and could not notice any  
201 significant difference from both sets of estimated tidal amplitudes at Brest. A drawback of the  
202 current T\_TIDE release is, however, that it cannot analyse datasets longer than one-year,  
203 whereas MAS is successfully applied over periods even longer than a century.

204 Table 1 shows the main tidal constituents that we obtained from the ocean-like tidal harmonic  
205 analysis performed on the tiltmeter observations that were previously corrected from the Earth  
206 tides over the period 2004/03/09 to 2005/07/18. The units are expressed in nano-radians.

207

208 **3.3 FES2004/NEA time modelling and sensitivity test distance**

209 The modelling is performed by combining FES2004 global oceanic model (Lyard *et al.*  
210 2004), and the refined NEA (North East Atlantic tidal solution) model in the close Atlantic  
211 and English Channel (Pairaud *et al.*, 2008).

212 We have plotted on figure 4 the modelled oceanic loading and the Earth Tide contribution, as  
213 well as the sum of these two signals and compared them with the observation. The chosen  
214 window permits to illustrate the best and the worst agreement. The largest discrepancies  
215 between modelled and observed oceanic loading occur for large tidal ranges. At the end of the  
216 window, during small tidal ranges, the agreement is far better (the whole time-series is  
217 available on request). In general, the EW component is better modelled than the NS  
218 component. This may be linked to the coast orientation (EW) which is located 2km  
219 northwards of the observing site.

220 We do not know the origin of these discrepancies and their variations in time. However, we  
221 form the hypothesis that it could come from the interference arrangement between the main  
222 tidal M2 group and the overtones (nonlinear harmonics). We only took into account 8 waves  
223 in the diurnal and semi-diurnal bands here and none of the non-linear tides. A further check  
224 will require to model the whole M4 group and even upper modes.

225 **Test distance**

226 We tested the spatial sensitivity of the tiltmeters. We have chosen an adapted geographical  
227 windowing, as in Boy *et al.* (2003) to represent the different contribution of several areas.  
228 This method splits the oceanic contribution into parts according to an adequate division of the  
229 geographical areas. The relevance of these areas is linked to the specificity of the local and  
230 regional coast contouring. The choice of the zones is partially arbitrary and is only for

231 discussion, but fundamentally also depends on the sensitivity of the method with respect to  
232 the distance, and hence on the power behaviour of the Green function:  $1/r$  for gravity and  $1/r^2$   
233 for tilts.

234 Three zones were considered (see Figure 5):

- 235 - Z1 corresponds to the English Channel (based on NEA model)  
236 - Z2 delimitate an intermediate zone (also based on NEA model)  
237 - Z3 is for the other parts of the world (using FES2004)

238 Figure 5 also shows M2 wave amplitude. Figure 6 shows the cumulative contributions of each  
239 of these 3 zones for all the diurnal and semi-diurnal waves.

240 In the semi-diurnal band (N2, M2, S2 and K2), we observe the effect of the local  
241 magnification of the corresponding group periods. Large zooms are required to see the further  
242 contribution; the local signal is definitely dominant.

243 The diurnal waves (O1, P1, K1, Q1) form a second class of patterns. Though the local zone  
244 (English Channel) dominates the signals, the Atlantic and remote zones are almost of the  
245 same order of magnitude and none of the contribution could be neglected. This is due to the  
246 fact that the diurnal waves are not amplified by the Channel

#### 247 **Discussion and Conclusions**

248 The sensitivity of the tilt method allows to observe the loading effect with a high signal/noise  
249 ratio. This implies that assuming a known mechanical response of the Earth, tiltmeters can be  
250 used to validate oceanographic models and nonlinear tides. Contrary to tide gauges whose  
251 spatial sensitivity is strictly local (and can be affected by the port configuration), the tilt offers  
252 an integrative measurement of the behaviour of the ocean with a regional spatial sensitivity.

253 They even could be more sensitive to coastal zones when tidal waves are magnified. This is  
254 the case for the M2 group; the wave amplitude is quickly decreasing when the distance to the  
255 coast increases, making the remote contribution really negligible.

256 The four main remaining issues are: 1) the difficulty to achieve a good accuracy in the  
257 calibration factor for this kind of tiltmeters, 2) the site effect, which is difficult to estimate in  
258 most cases, 3) the lack of atmospheric detailed data to correct from pressure within this short  
259 period band, and 4) the necessity to take into account a dynamical and coupled atmosphere-  
260 ocean modelling (see Boy *et al.*, this issue). However, these issues can be tackled in a near  
261 future. New experiments are carried on in Brittany near Ploemeur in France (Bour *et al.*,  
262 2008) which could serve to improve our knowledge. Indeed, long-base hydrostatic tiltmeters  
263 have been set up in shallow galleries. They have been recording for a few months. Both  
264 calibration uncertainties and site effects will be easier to solve there for that kind of  
265 instruments. In parallel, atmospheric sampling rates and coupled modelling with the oceans  
266 are continuously improving.

267 Due to its features and assuming further improvements, tilt could become a systematic tool to  
268 test oceanic models as far as non linear high harmonics are concerned. Neither gravity nor  
269 GPS techniques are able to see M4, M6, M8 and M10 waves with such a signal/noise ratio as  
270 the one reached by tiltmeters today.

271 **Acknowledgement**

272

273 We thank Marie-France Esnoult and Karim Mahiouz for installing the tilt-meters, Jacques  
274 Delorme and the French Marine for providing the Roule gallery to install the tilt-meters. We  
275 would also like to thank Bernard Simon (SHOM) for kindly providing us his tools (MAS) in  
276 order to apply the ocean tidal-like analyses to the tiltmeter records. This study has been

277 supported by the program CNRS-DBT and the grant in the frame of the multi-organisation  
278 GDR-G2. Nicolas Florsch is currently welcomed at the Department of Mathematics and  
279 Applied Mathematics at Cape Town University, South Africa, and is granted by the French  
280 Organization “Institut de Recherche pour le Développement”. Jean-Paul Boy is currently  
281 visiting NASA Goddard Space Flight Center, with a Marie Curie International Outgoing  
282 Fellowship (N° PIOF-GA-2008-221753).

283 **References**

- 284 Blum, P., 1962. Contribution à l'étude des variations de la verticale en un lieu, Ann.  
285 Geophys., 19, 215–243.
- 286 Boy, J.P., Llubes, M., Hinderer, J., and Florsch, N., 2003. A comparison of tidal ocean  
287 loading models using superconducting gravimeter data. JGR, vol. 108, n°B4.
- 288
- 289 Boy, J.-P., M. Llubes, R. Ray, J. Hinderer, N. Florsch, S. Rosat, F. Lyard and T. Letellier,  
290 2004, Non-linear oceanic tides observed by superconducting gravimeters in Europe, J.  
291 Geodyn., 38, 391-405.
- 292
- 293 Braitenberg.C., and Zadro, M., 1999. The Grotta Gigante horizontal pendulums -  
294 instrumentation and observations. Bollettino di Geofisica Teorica ed Applicata, 40 , no 3-4,  
295 pp. 577-582.
- 296
- 297 Cartwright, D.E., and Ray, R.D., 1990. Oceanic tides from Geosat altimetry. J. Geophys.  
298 Res., 95 (C3), pp. 3069–3090.
- 299

- 300 Farrell, W., 1977. Deformation of the Earth by surface load, Review of Geophysics Space  
301 Physics, 10(3), 761–797.
- 302 Harrison, J. C., 1976. Cavity and topographic effects in tilt and strain measurements. J.  
303 Geophys. Res., 81, 319 – 328
- 304
- 305 Itsueli, U.J., Bilham, R.G., Goultby, N.R., and King, G.C.P., 1975. Tidal strain enhancement  
306 observed across a tunnel, *Geophys. J. R. astr.Soc.*, **42**, 555
- 307
- 308 King, G., Zürn, W., Evans, R., Emeter, D., 1976. Site Correction for Long Period  
309 Seismometers, Tiltmeters and Strainmeters. Geophysical Journal International, vol. 44, issue  
310 2, pp. 405-411.
- 311 Kroner, C., Jahr, T., Kuhlmann, S., & Fisher, K., 2005. Pressure-induced noise on horizontal  
312 seismometer strainmeter records evaluated by finite element modelling, *Geophys. J. Int.*, 161,  
313 167–178.
- 314 Lecolazet, R. & Wittlinger, G., 1974. Sur l'influence perturbatrice de la deformation des  
315 cavités d'observation sur les marées clinométriques, *C. R. Acad. Sc. Paris*, 278, 663–666.
- 316 M. Llubes, N. Florsch, J.P. Boy, M. Amalvict, P. Bonnefond, M.N. Bouin, S. Durand, M.F.  
317 Esnoult, P. Exertier, J. Hinderer, M.F. Lalancette, F. Masson, L. Morel, J. Nicolas, M.  
318 Vergnolles, G. Wöppelmann, 2008. Multi-technique monitoring of ocean tide loading in  
319 Northern France. *Compte-rendus Géosciences*, *C. R. Geoscience* 340, 379–389
- 320
- 321 Llubes, M., Florsch, N., , Amalvict, , M., Hinderer, J., Lalancette, M.F., Orseau, D., et Simon,  
322 B., 2001. Observation gravimétrique des surcharges océaniques : premières expériences en  
323 Bretagne. *C.R. Acad. Sci, Earth and Planetary Sciences* 332, 77-82.

- 324 Melchior, P., 1983. The Tides of the Planet Earth, Pergamon Pr.
- 325 Pagiatakis, S., 1990. The response of a realistic Earth to ocean tide loading, Geophys. J. Int.,  
326 103, 541–560. DOI: 10.1111/j.1365-246X.1990.tb01790.x
- 327 Pawlowicz, R., Beardsley, B., and Lentz, S., 2002. Classical tidal harmonic analysis error  
328 estimates in MATLAB using T\_TIDE. Comput. Geosci. 28, 929–937.
- 329 Pouvreau, N., Martin Miguez, B., Simon, B, and Woppelmann, G., 2006. Evolution of the  
330 tidal semi-diurnal constituent M2 at Brest from 1846 to 2005. C. R. Geoscience, 338, pp.  
331 802–808.
- 332 Rerolle, T. , Florsch, N., Llubes, M., Boudin, F., and Longueverg,e, L., Inclinometry, a new  
333 tool for the monitoring of aquifers? C. R. Geoscience 338 (2006).
- 334 [doi:10.1016/j.crte.2006.07.004](https://doi.org/10.1016/j.crte.2006.07.004)
- 335 B. Saleh, P.A. Blum and H. Delorme, New silica compact tiltmeter for deformations  
336 measurements, J. Survey Eng. 117 (1991), pp. 27–35.
- 337 Simon, B, 2007. La marée oceanique côtière. Collection “Synthèses”, Ed. Insitut  
338 Océanographique, 433 pp.
- 339
- 340 Vey,S. , Calais, E., , Llubes, M., Florsch, N., Woppelmann, G., Hinderer, J., Amalvict, M.,  
341 Lalancette, M.F., Simon, B., Duquenn F., Haase, F.S., 2002 GPS measurements of ocean  
342 loading and its impact on zenith tropospheric delay estimates: a case study in Brittany,  
343 France. Journal of Geodesy, vol. 76, 8, pp 419-427.
- 344
- 345

346 **Figure captions:**

347

348 Figure1 : Site location and installation of a Blum Pendulum in the “Souterrain du Roule” at  
349 Cherbourg

350

351 Figure2 : EW and NS raw and band-pass filtered tilt records at Cherbourg

352

353 Figure 3 : Fourier analysis (periodogramms) of the tilt records reveal a high signal/noise ratio  
354 of 100 (40 dB) at 2 cycle/day. It detect peaks till the 1/10 diurnal cycle.

355

356 Figure 4: on the bottom part, Earth tide and loading models are shown separately, while there  
357 are summed in the top part of the figure. In both cases, the observation is also plotted and  
358 shows a greater amplitude than the model. The misfit could be due to non-linear tides that are  
359 not included in this computation.

360

361 Figure5 : The computation is performed by distinguishing three exclusive zones: this enables  
362 to study the influence of close, intermediate and distant oceanic loading effects. Zone 1: from  
363 -5° to 1.5° in long and 48.5° to 51.25° in lat; Zone 2: from -20° to 14° in long and 30° to  
364 61° in lat (excluding Z1); Zone 3: global excluding Z1 and Z2. In Z1 and Z2 the North-East  
365 Atlantic (NEA) tidal solution (Pairaud et al., 2008) is used, while Z3 is computed by using  
366 FES2004 model (Lyard et.al., 2006).

367

368 Figure 6: Cumulative contribution of the 3 different zones for all diurnal and semi-diurnal  
369 waves.

370

371 Table 1 : Results from the ocean-like tidal harmonic analysis applied to the tiltmeter  
 372 observations (2004/03/09-2005/07/18) previously corrected for the Earth tides.

Tidal constituent	ALPHABETICAL DOODSON NR.	Amplitude East-West (in nano-radians)	Amplitude North-South (in nano-radians)
M2	BZZZZZZ	435	404
S2	BBXZZZZ	149	141
N2	BYZAZZZ	85	82
K2	BBZZZZZ	41	40
K1	AAZZZZA	34	23
O1	AYZZZZY	19	6
P1	AAXZZZY	11	6
Q1	AXZAZZY	1	10
M4	DZZZZZZ	12	32
MS4	DBXZZZZ	8	20
MN4	DYZAZZZ	4	10
M6	FZZZZZZ	3	7
2MS6	FBXZZZZ	3	8
2MN6	FYZAZZZ	2	5
5MS8	HXBZZZZ	1	6

**Figure 1**



**Figure 2 :**

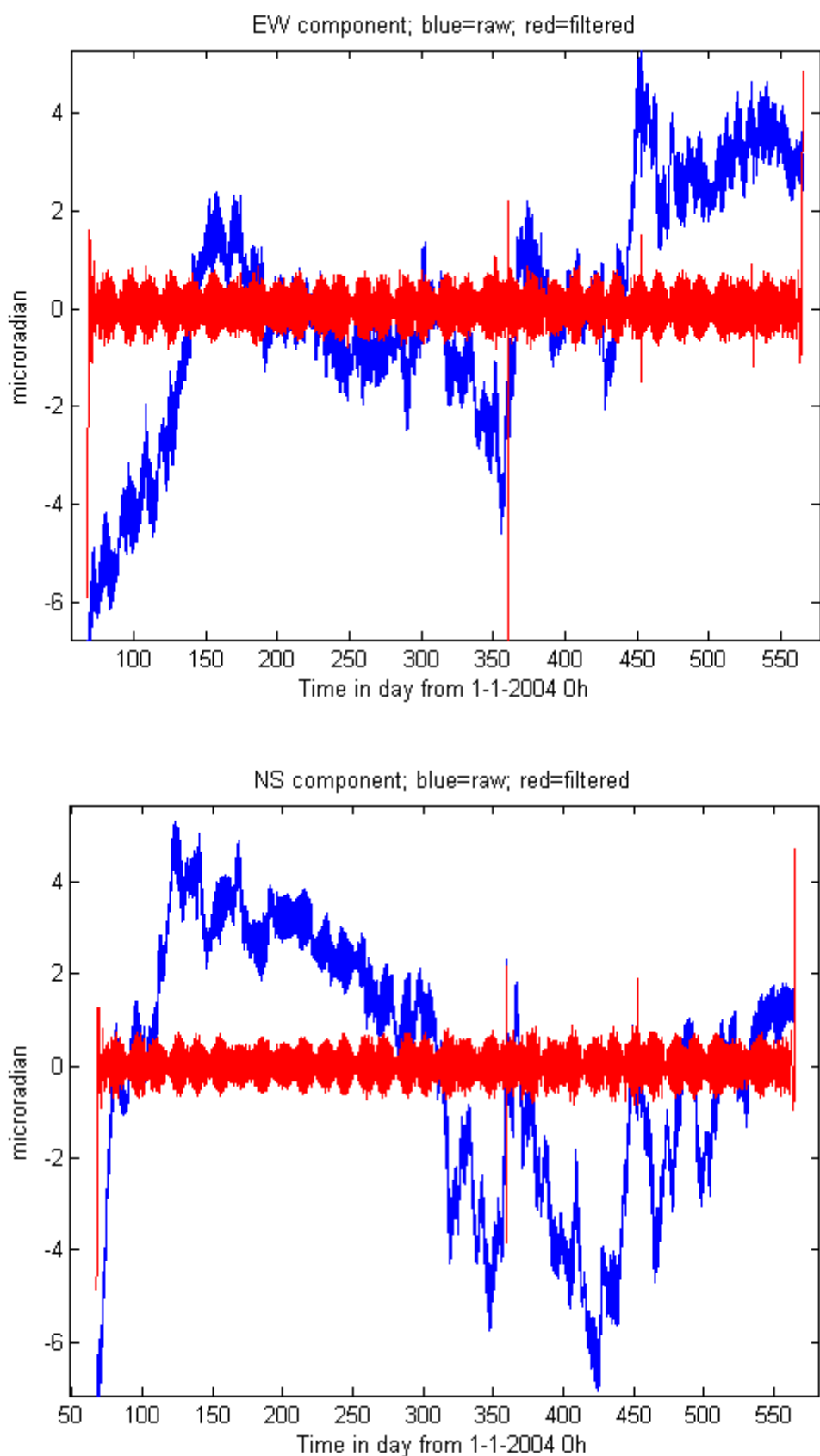


**Figure 3**

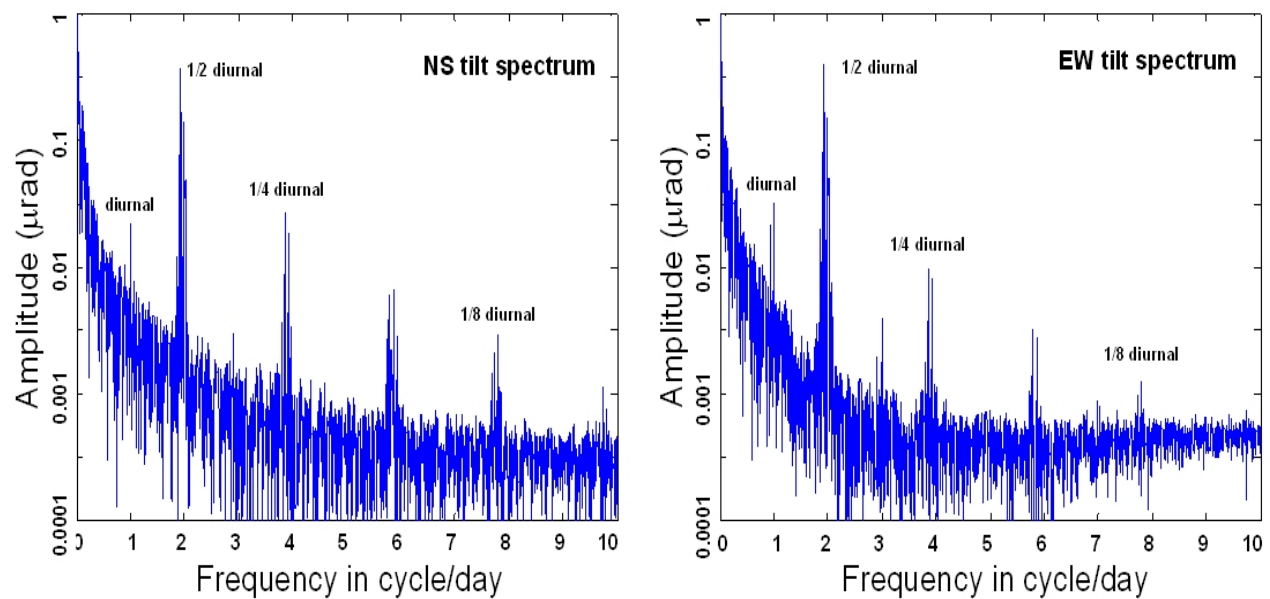


**Figure 4**

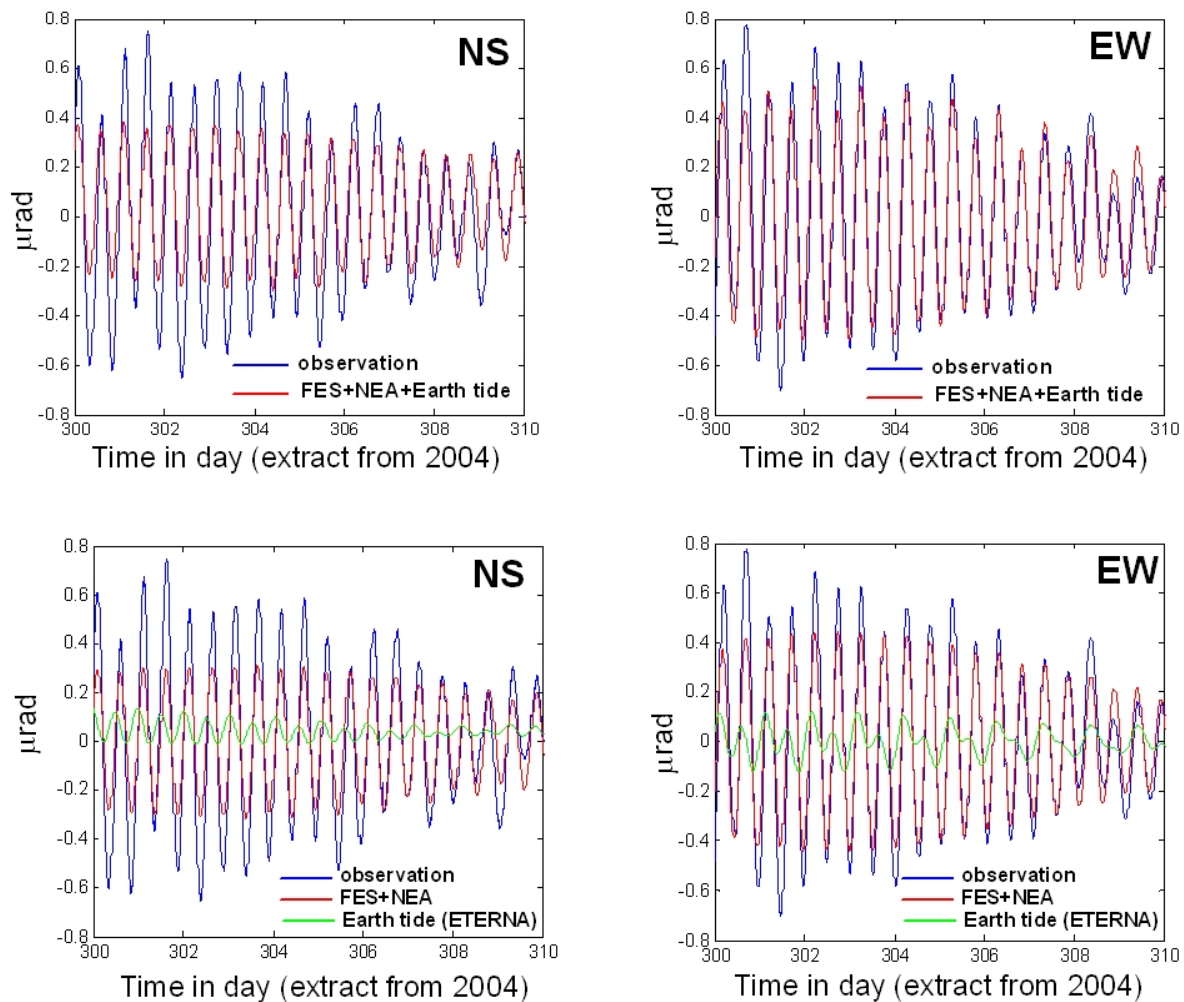


**Figure 5**

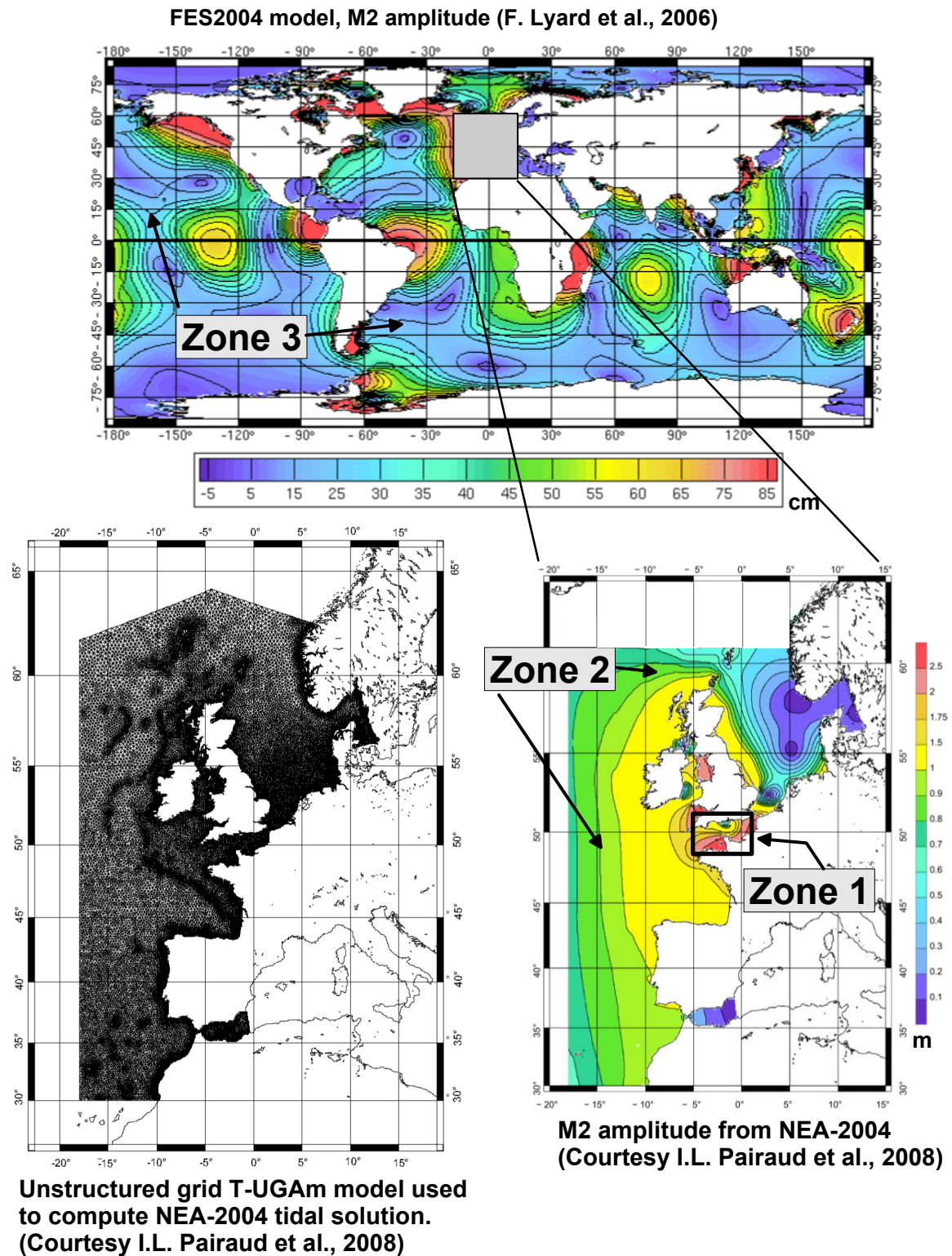


**Figure 6**

